Exploring the visual system of the black Grouse (*Lyrurus tetrix*): Combining experimental and molecular approaches to inform strategies for reducing collisions

Simon Potier[1*], Jean-Marc Lassance[2], Constance Blary[3], Justine Coulombier[4], Sandrine Berthillot[4], Virginie Dos Santos[5], Christine Andraud[6] and Marjorie A. Liénard[7*]

1 Simon Potier Expert Scientifique, Foucrainville, France

2 Laboratory of Evolutionary Neuroethology, GIGA Institute, University of Liège, Belgium

3 CEFE, Univ Montpellier, CNRS, EPHE, IRD, Montpellier, France

4 Parc National de la Vanoise, Vanoise, France

5 Association Observatoire des Galliformes de Montagne, Sevrier, France

6 Centre de Recherche sur la Conservation des Collections, CNRS, Muséum National d'Histoire Naturelle, France

7 Laboratory of Molecular Biology of Sensory Systems, GIGA Institute, University of Liège, Belgium; Department of Biology, Lund University, Sweden

Corresponding authors
*sim.potier@gmail.com; marjorie.lienard@uliege.be

ORCID IDs:

S.P.: 0000-0003-3156-7846
J-M.L.: 0000-0002-3675-6956
C.B.: 0000-0001-6204-9983
C.A.: 0000-0002-3112-9363
M.A.L.: 0000-0003-3193-3666

Keywords: visual acuity, contrast vision, bird ecology, spectral sensitivity, opsin

Abstract

Understanding the visual systems of birds can inform conservation efforts and mitigate anthropogenic threats, such as collisions with man-made structures. This study investigates the visual abilities of the black grouse (*Lyrurus tetrix*), a European mountain bird highly vulnerable to collisions. Using an integrative approach, we assessed key visual components including visual field configuration, spatial resolution, contrast sensitivity, and spectral sensitivity. Behavioral assays revealed that black grouse have an extensive visual field with a wide binocular overlap and minimal blind spots, allowing for efficient predator detection and foraging. However, their spatial resolution and contrast sensitivity are relatively low, consistent with other prey species. Molecular analyses identified four cone opsins (SWS1, SWS2, Rh2, and LW) with spectral sensitivities spanning ultraviolet to long wavelengths (393–546 nm). These findings highlight the black grouse's ability to detect UV light. Our results emphasize the need for collision mitigation measures tailored to species-specific visual abilities, including diverters designed with enhanced reflectance and increased visibility. This study advances our understanding of avian vision and provides critical insights to guide conservation strategies for reducing bird collisions in alpine habitats.

Introduction

Vision represents a major sensory modality in avian species, allowing most modern birds to collect accurate and instantaneous environmental information from different directions and over varying distances, and to perform tasks such as foraging or predator detection (Land & Nilsson, 2012, Martin, 2017). These tasks rely on optimised spatial acuity, *i.e.* the perception of spatial details, and the ability for the visual system to resolve images, hence eye size is a generally strong predictor of visual acuity in birds (Caves et al., 2024). While eyes are metabolically expensive organs and therefore usually physically constrained (Witter & Cuthill, 1993, Laughlin et al., 1998, Niven & Laughlin, 2008, Moran et al., 2015), most birds investigated to date typically have larger eyes relative to body mass (Brooke et al., 1999, Caves et al., 2024), as well as relatively more complex retinae (Meyer, 1977, Goldsmith, 1990, Martin, 2022) than other terrestrial vertebrates. Avian photoreceptors absorb photons of light in the retina, which then, to form images, sample visual information projected by the lens and cornea (Martin, 1984, Martin, 2022). Differences in visual abilities result from differences in eye morphology that meet species-specific ecological requirements (Martin, 2022), shaping

sophisticated detection, recognition and discrimination of objects to guide remarkable and vital behaviours such as navigation, foraging and communication.

To do it efficiently, birds need to be able to gather environmental visual information and spot a target of interest, which requires an optimal visual field (Martin, 2017). The visual field describes the volume of space around the head from which visual information can be gathered. The fields of view vary significantly among species (Martin, 2017, Potier et al., 2018a, Cantlay et al., 2023), and are associated with different foraging, parental care, predator detection and sociality in birds (Martin, 2014). However, the visual field is in trade-off with other visual abilities needed for spotting, such as spatial resolution. For instance, old world passerine birds (Emberizidae) that have larger binocular overlap, that is the portion of the world around an animal's head viewed simultaneously by its two eyes, seemed to have lower spatial resolution (Moore et al., 2015). Reversely, predatory and scavenging species from open habitats typically display higher spatial resolution (Caves et al., 2024). In addition to spatial resolution, target detection requires the ability to discern contrasts (*i.e.* contrast sensitivity). Generally, birds have relatively low contrast sensitivity (Blary et al., 2024). Phylogeny tends to explain around 25% of variation in birds (Blary et al., 2024), suggesting that ecological factors such as foraging may be a driver of contrast sensitivity. When a target is in movement, the temporal resolution is also an important component for detection, that can vary over 3 degrees of magnitude among species (Potier et al., 2020a).

Finally, differences in spectral photoreceptor sensitivity among bird species are shaped by a combination of ecological drivers such as diel activity patterns (Wu et al., 2016), foraging strategies (Odeen & Håstad, 2010, Wu et al., 2016), sexual selection, predator-prey interactions or social signaling (Outomuro et al., 2017, Cooney et al., 2019). Combined, these factors contribute to the evolution of diverse specialized visual systems finely tuned to each species' natural history, ecological niche and behavioral needs. In particular, bird retinas contain multiple types of photoreceptors, including single types of rod and double-cone photoreceptors, as well as four types of single cones each typically expressing distinct visual opsin pigments. Rhodopsin (Rh1) is mostly expressed in rods, the vertebrate photoreceptor type adapted to detect dim-light levels and is more abundant in nocturnal birds (Ruggeri et al., 2010, Potier et al., 2020b). Cone opsins, on the other hand, dominate the retina of diurnal birds to achieve spectral resolution across a broad light spectrum, and typically confer tetrachromatic colour vision in the majority of species investigated to date (Kelber, 2019, Martin, 2022, Wu et al.,

2016). Molecular variation between opsin subtypes conveys species-specific maximal spectral sensitivities (λ_{max}) (Hauser & Chang, 2017, Hagen et al., 2023), which together with interspecific molecular tuning changes within opsin subtypes, further convey large differences in underlying visual pigment λ_{max} (Frentiu & Briscoe, 2008, Carvalho et al., 2007b, Aidala et al., 2012, van Hazel et al., 2013, Hauser et al., 2014).

Bird short-wavelength opsins type 1 (SWS1) occur in two types, ranging in maximal spectral sensitivity from ultraviolet (<400 nm) to violet (400-430 m) part of the spectrum (Hunt et al., 2007, Carvalho et al., 2007a, Carvalho et al., 2011, Hauser et al., 2014). Given the significance of UV signalling in visual ecology, research around understanding sensitivity to short-wavelengths has led to identify evolutionary trajectories and unique molecular mechanisms amongst vertebrates that involve several spectral residues that contribute to expand bird SWS1 absorption spectrum across the UV-Violet range (Hart & Hunt, 2007, Hauser et al., 2014, Hagen et al., 2023). Short wavelength opsins type 2 (SWS2) typically absorb maximally between 430-460 nm, middle wavelength sensitive opsins (MWS or Rh2) absorb light in the range 470-510 nm, and long wavelength opsins subtypes absorb light between 530-560 nm. Bird cones, alike those of lizards and turtles (Borges et al., 2015, Corredor et al., 2022, Hagen et al., 2023) contain carotenoid-rich coloured oil droplets functioning as short-wavelength cut-off light filters, which can modulate the associated photoreceptor spectral sensitivity of single cones generally shifting peak sensitivity to longer wavelengths (Hart, 2001, Knott et al., 2010, Toomey et al., 2015, Lim & Pike, 2016).

Identifying and integrating species-specific optical, behavioural and molecular characteristics of bird visual systems can reveal subtle differences that contribute to confer finely tuned adaptations involved in a species ecology.

These insights may also inform on a system's physical or physiological limitations that may impact visually guided behaviours in a variety of natural and perturbed environments. Collisions represent a major source of anthropogenic mortality which kills millions of birds worldwide every year (Marques et al., 2014, Bernardino et al., 2018), and studying the visual system and behaviour of birds contributes to inform on reducing it (Martin, 2011a, Martin, 2022, Martin & Banks, 2023). An additional source of collision lies in the creation and expansion of ski areas, which have been identified as a major cause of population decline in mountain birds (Buffet & Dumont-Dayot, 2013).

Among European mountain birds, the black grouse, *Lyrurus tetrix,* represents 70% of bird mortality due to collision, notably in the French alps (Buffet & Dumont-Dayot, 2013),

which readily represented 476 individuals in an earlier 4-year survey (Bech et al., 2012) although this number is likely underestimated . To reduce collision, a number of bird diverters have been developed, with different efficiency depending on types and bird species (Ferrer et al., 2020). One of the reasons might be that the designs of bird diverters have been based on the perception of humans and on engineering considerations but not on the perception of birds (Martin, 2022). Therefore, it is crucial to understand specific visual behaviour and perception abilities of species suffering from collision, which could contribute to design alternative effective visual diverters and improve conservation in natural areas.

In this study, we use an integrative approach and range of experimental techniques to determine the visual abilities of the black grouse and better understand the system's requirements to detect visual objects. We analysed reflex-like and ophthalmoscopic behaviours to characterize different components including the visual field, spatial resolution and contrast sensitivity. We then performed a profiling of cone opsin genes via RNA-sequencing and determined SWS1, SWS2, MWS and LWS opsin cone spectral sensitivities via heterologous expression and UV-VIS analyses. Next, we integrate morphological, experimental and molecular analyses to define visual diverters detectability, taking into account visual constraints such as oil droplets on spectral sensitivity. Altogether, our results provide a more comprehensive analysis of the blackgrouse visual abilities to better inform conservation biology initiatives.

Material and methods

(a) Contrast sensitivity

(i) *Lyrurus tetrix* birds and study location

Two 4-month-old male black grouse (*Lyrurus tetrix,* Phasianidae) individuals belonging to the breeding centre of Frank Grosemans (Belgium) were used to study contrast sensitivity. The experiments were run on site on October 5, 2022.

(ii) Experimental set-up

We used a reflex-like behaviour setup to study the contrast sensitivity of each individual, following Wagner et al. (Wagner et al., 2022) and Blary et al. (Blary et al., 2024), which give similar peak contrast sensitivities but not their associated spatial frequency than operant conditioning method (Blary et al., 2024). These reflexes or nystagmus are caused by involuntary

compensatory mechanisms for image stabilization, *i.e.,* the individual follows the moving object by eyes to keep the image stationary on the retina (Wagner et al., 2022). Because most birds have limited eye movements (between 2 and 18°) (Martin, 2009, O'Rourke et al., 2010), they follow the object with large head movements. To estimate the optocollic reflex (hereafter called "OCR"), birds were placed into a transparent U-shaped box adapted to the size of the species (L60 x W40 x H44 cm), with a black wooden floor and ceiling, and a 3 mm thick polycarbonate wall. The polycarbonate wall allowed the bird to see the stimulus, without influencing the visual abilities (Blary et al., 2024). The ceiling was made of two wooden boards spaced 5 cm apart: a perforated panel to let the air pass through and a solid and smaller panel so that the bird could not see through the holes of the other panel. All wooden surfaces were painted matte black (Liberty black, mat, GoodHome). A wooden door placed at the back of the box allowed to position the bird in the box. The experimental box was placed at the centre of an octagon of a radius of 69cm made with computer monitors (Acer KG1 Series, 28 inches (62x34 cm), 4K 3840x2160 pixels, 60 Hz, Acer Inc. Taiwan), in portrait orientation, with the centre placed on the same level as the birds' head (Figure 1). The stimulus covered 236x46 degrees of the visual field (horizontal x vertical extent). This layout covered enough of the bird's visual field to elicit an OCR (Schmid & Wildsoet, 1998, Blary et al., 2024).

The monitors and the bird were placed in an opaque black cloth tent 300 cm length x 300 cm width x 250 cm high with the base of monitors and the floor also covered by an opaque black cloth to minimize possible disturbing external visual signals. The experimenter stayed outside the tent during the entire experiment. One video camera (25 frames per second; Sony DCR-SR55 HD) placed above the monitors, allowed recording the bird's behaviour during the experiment. In addition, a smartphone (Iphone 13, Apple) connected to a screen located outside the tent was used so that the experimenter could monitor the bird during the entire procedure.

(iii) Stimuli

The stimuli were generated in Matlab (R2021) using Psychtoolbox (Brainard, 1997). The computer monitors were connected to a MacbookPro (Apple) using a HDMI splitter (8-Port, 4K, 60Hz, ST128HD20, StarTech). The stimuli consisted of vertical sinusoidal achromatic gratings at variable spatial frequency and contrast. The angular velocity was set at 20 degrees per second, similarly to closely related species (Blary et al., 2024). Six spatial frequencies were used (0.47, 0.56, 0.85, 1.06, 1.27 and 1.59 c/deg) and Michelson contrast ranged from 0.012 and 0.99 (Table S1) to obtain the contrast sensitivity function (CSF), *i.e.* the peak contrast

sensitivity along with the corresponding spatial frequency and the high cut-off frequency (*i.e.* the highest SF perceived by the individual at a Michelson contrast of 1). Michelson contrast is defined as:

$$Michelson\ contrast = \frac{I_{max} - I_{min}}{I_{max} + I_{min}}$$

where I_{max} and I_{max} represent the highest and lowest luminance. For each contrast level tested, the contrast was evaluated by measuring the difference in luminance between the darkest and lightest area of the grating in cd m^{-2} at the centre of the monitor with a luxmeter (Hagner ScreenMaster, B. Hagner, Sweden).

The stimulus was shown on monitors for 20 seconds (Schmid & Wildsoet, 1998, Shi & Stell, 2013, Wagner et al., 2022, Blary et al., 2024). The direction of the stimulus (clockwise or counter-clockwise) was changed in a pseudo-random order, *i.e.* the number of consecutive trials in the same direction was limited to three. The illuminance at the bird's head was measured with the luxmeter: 110 lux inside the U-shaped box and 321 lux inside the cylinder. The stimulus brightness was 73 cd m^{-2}.

(iv) Experimental procedure

Computer monitors were turned on 20 minutes before the beginning of the experiment so that they reached maximum brightness. The experimental session started 10 minutes after the bird was placed in the device to allow a habituation phase. The presence of OCR was assessed "by eye" by the experimenter (Schmid & Wildsoet, 1998, Shi & Stell, 2013, Blary et al., 2024). Each session began with maximum contrast (Michelson contrast = 0.99) to ensure that the bird was expressing an OCR detectable by the experimenter. The contrast was then decreased and increased in a stepwise manner to approach the contrast threshold where birds no longer exhibited the reflex. Each trial consisted of a specific combination of spatial frequency and contrast, separated by 5 seconds (or longer if the bird did not look at monitors) during which an isoluminant homogeneous grey was displayed on monitors. We used the "four of five" criteria, *i.e.* each specific combination was presented 5 times and the response was considered reliable if the OCR was elicited at least 4 times out of the 5 trials (Shi & Stell, 2013, Blary et al., 2024). Thus, the lowest contrast with a validated 4 out of 5 criterion was defined as the threshold contrast. Once this threshold was reached, the experiment was repeated with the same angular

velocity but with a different spatial frequency. The experimenter was able to view the trials post hoc and validate or not the presence of OCR and used the results from the blind double-checked for the analyses.

(b) Visual field

(i) Birds and study location

Experiments were performed on October 6, 2022 on the same individuals used in (a) at the breeding centre of Frank Grosemans (Belgium).

(ii) Experimental procedure

We used a non-invasive procedure to measure visual field characteristics in alert birds, described extensively in multiple previous papers (Fernandez-juricic et al., 2008, Martin, 2007, Potier et al., 2016b, Potier et al., 2017). In summary, each bird was held firmly for 20-30 min in a plastic restraining tube of the appropriate size to avoid any movement. The bird's legs were gently immobilized with light tape (Micropore Surgical tape 1530/1B) together and cushioned by foam rubber held between them. The head was held at the centre of a visual field apparatus (a device that permits the eyes to be examined from known positions around the head) by a specially manufactured steel and aluminium bill holder. The head was maintained in the visual field apparatus following the natural head position of the birds. The surfaces of the bill holder were coated in cured silicone sealant to provide a non-slip cushioned surface. We held the bill in place with Micropore tape, being sure not to cover the nostrils to allow for breathing. We took calibrated photographs of the head and the eyes of each bird while held in the apparatus to determine eye positions within the skull, the horizontal separation between the centre of the two eyes, the distance between the centre of the eye and the bill tip, and the bill length.

Visual field parameters were measured using an ophthalmoscopic reflex technique. The perimeter's coordinate system followed conventional latitude and longitude measures, with the equator aligned vertically in the median sagittal plane of the head (i.e., a vertical plane that divides the head symmetrically into left and right hemisphere). We used this coordinate system in the presentation of the results. We examined the eyes using an ophthalmoscope mounted against the perimeter arm with an accuracy of ± 0.5°. We measured the boundaries of the retina projection by the positions that the eyes spontaneously adopted when they were fully rotated

‘forwards’ (converged for estimation of binocular area boundaries) and ‘backwards’ (diverged for estimations of the blind sectors boundaries) for the blind area behind the head. We did not measure the degree of eye movements or the projection of the pecten to reduce the time the animals were restrained.

We corrected our data for viewing from a hypothetical viewing point placed at infinity. This correction is based upon the distance used in the measurements taken with the visual field apparatus and the horizontal separation of the eyes (Martin, 1984). After the corrections, we constructed a topographical map of the visual field and its different components. These features included lateral fields, binocular field, cyclopean field (the total field around the head produced by the combination of the monocular fields of both eyes), and blind areas above and behind the head. The limits of the visual field were determined at 10° intervals of elevation in an arc from directly behind the head, to above the head, and then down to 50° below the horizontal in front of the head. We did not record data at elevations where the bill holder was blocking our view and instead estimated the binocular field width as the mean value of the binocular field widths immediately above and below these elevations (Martin, 2017).

(c) Eye size and visual acuity

We estimated the spatial resolving power of the eye based on Corneal Diameter (CD) from the calibrated photographs (Spiegel et al., 2013, Potier et al., 2016a, Potier et al., 2017) Corneal diameters were measured with ImageJ 1.41 and then translated to Axial Length (AL) using the formula for diurnal animals (Hall & Ross, 2007):

$$AL = \frac{CD}{10^{-0.22}}$$

We then calculated the spatial resolution (SR) using the following function derived from (Caves et al., 2024):

$$SR = 10^{(0.26 + 0.81 * log_{10}(AL))}$$

(d) Opsin spectral sensitivity

(i) Collection of eye tissues and extraction of ribonucleic acid (RNA).

Ocular tissue, including the retina, was dissected by a veterinarian from an adult individual black grouse *L. tetrix,* from the Vanoise park in France (ID: JB-2021-E001, POIA Project Vanoise), respecting permits in place. The collected tissue was directly preserved in DNA/RNA reagent (Zymo Research) and stored at -20° C. The tissue was removed from the preserving reagent, quickly dried and subsequently ground to a fine powder in liquid nitrogen in a mortar, and, then processed for RNA extraction following the procedure described in the Monarch Total RNA miniprep kit (NEB). The integrity of the RNA was evaluated using a bioanalyzer and the quantity assessed using Qubit high sensitivity RNA.

(ii) cDNA libraries and RNA-sequencing.

Five hundred micrograms of high-quality RNA were used to prepare a deoxyribonucleic acid (DNA) library following the protocol detailed in NEBNext Ultra II Directional RNA library prep kit for Illumina (NEB), including the following specifications: selection of messenger RNA (mRNA), a selected average size of 500 base pairs for fragmentation, and the addition of Illumina adapters. cDNA library quality was evaluated by bioanalyzer as well as by quantitative PCR (Polymerase chain reaction). Paired-end sequencing (2x150bp) was performed on an Illumina NovaSeq6000 equipped with an S4 flowcell (NovaSeq Control Software 1.8.0/RTA v3.4.4, SciLifeLab, Stockholm, Sweden). In total, we obtained 197.8 million read pairs. The transcriptome sequencing data have been deposited into the European Nucleotide Archive (ENA) under the accession number xx.

(iii) Pre-assembly filtering

Raw reads were first preprocessed by correcting and excluding aberrant reads using the k-mer-based read-error correction tool Rcorrector (Song & Florea, 2015). We next proceeded to adapter removal and quality trimming (--quality-cutoff=20) using cutadapt version 4.2 (Martin, 2011b). During that step, we also removed read pairs with either read shorter than 36 bp. Next, we removed reads corresponding to rRNA sequences by mapping the reads against a custom database built from SILVA SSU and LSU datasets (release 138.1)(Quast et al., 2013) using bowtie2 (Langmead & Salzberg, 2012). Finally, reads corresponding to mitochondrial sequence were extracted using MITGARD (Nachtigall et al., 2021). The final set of assembly-ready reads contained 173.8 million read pairs.

(iv) *De novo* transcriptome assembly and annotation

De novo assembly of the pre-processed paired-end reads was performed using Trinity v2.14.0 (Grabherr et al., 2011) with default parameters. Completeness of the assembly was assessed with BUSCO v3.0.2 (Simão et al., 2015) using the Vertebrata and Aves datasets. We applied the pipeline implemented in Trinotate v3.2.1 (Bryant et al., 2017) to predict candidate protein coding regions within transcript sequences using TransDecoder v5.5.0 (https://github.com/TransDecoder/TransDecoder) and to generate a functional annotation of the transcriptome data. We retrieved full-length candidate opsin transcripts from the resulting annotation table.

(v) Expression estimates

We obtained expression estimates using RSEM v1.3.0 (Li & Dewey, 2011). First, we generated a transcript to gene mapping file from the Trinity output using the dedicated script from the RSEM package. Next, quality-trimmed paired-end reads were aligned to the transcriptome using Bowtie2 v2.4.1 (Langmead & Salzberg, 2012). The overall alignment rate was 85.29%. Finally, RSEM was used to compute the expression estimates.

(vi) Opsin functional expression

Opsin-specific oligonucleotide primers (Table S2) encompassing two distinct restriction sites were designed to amplify the coding region of each identified visual opsin (SWS1, SWS2, RH2, LW) by PCR using retinal cDNA synthesized using the GoScript protocol (Promega) as template. After verification by agarose gel electrophoresis, expected amplified product sizes were gel-purified using the Monarch DNA gel extraction kit (NEB), digested with restriction enzymes, subcloned into the linearized pcDNA5-FLAG-T2A-mruby2 expression vector (Liénard et al., 2021), and propagated into a Q5 strain of *Escherichia coli* bacteria (NEB). After incubation of individual bacterial colonies in Luria-Broth culture medium containing ampicillin, DNA plasmids were purified, and each construct sequence was verified by Sanger sequencing. A stock of each final plasmid was prepared following the ZymoPURE II Plasmid MidiPrep kit protocol (Zymo, D4200) to obtain a quantity of 480 micrograms.

(vii) Protein purification, absorbance measurement and UV-VIS analyses

Each plasmid was transfected into human embryonic kidney cells (HEK293T) following the PASHE procedure (Liénard et al., 2022). Briefly, *11*, cis-retinal, was added in solution in the dark (under red light) 6h post transfection. Cells were collected and the total membrane fraction solubilized using n-Dodecyl-D-Maltoside detergent (DDM) 48h after transfection, and the

opsin fraction bound to FLAG resin and incubated overnight. The next day, the opsin-FLAG complex was purified and eluted using FLAG peptide, then concentrated by centrifugation at 4000 rpm and 4°C for 50 min prior to ultraviolet-visible (UV-VIS) spectroscopy. Rhodopsin (opsin in complex with the chromophore) thus purified in solution, and adapted to the dark, was measured in the dark from 1.5 µL aliquots using a UV-VIS spectrophotometer NanoDrop 2000/2000c (Thermo Fisher). For each rhodopsin, we obtained estimates of lambda max by nonlinear fitting to absorbance data according to a visual model (Govardovskii et al., 2000) and performed 1000 bootstrap replications to calculate lambda max predictions and confidence intervals (Liénard et al., 2022) in R v. 3.6.6. using the rsample (Frick et al., 2022) and tidymodels (Kuhn & Wickham, 2020) packages.

Results

(a) Black grouse visual field

The maximum binocular overlap was 40°, which pointed 30° above the eye bill-tip direction (Figure 1). At rest, black grouse have a binocular overlap of 28° and a blind spot of only 7° behind the head (Figure 1). The vertical extent of the binocular field in the median sagittal plane was 170° and extended 40° behind from directly above the head to the horizontal (Figure 1). The binocular field width from directly above the head to the horizontal was 6°. Lateral placement of the eyes in the skull, coupled with wide monocular fields and small blind spot provides a large cyclopean field, i.e. the full extent of the volume of space around the head that at any one instant can provide visual information.

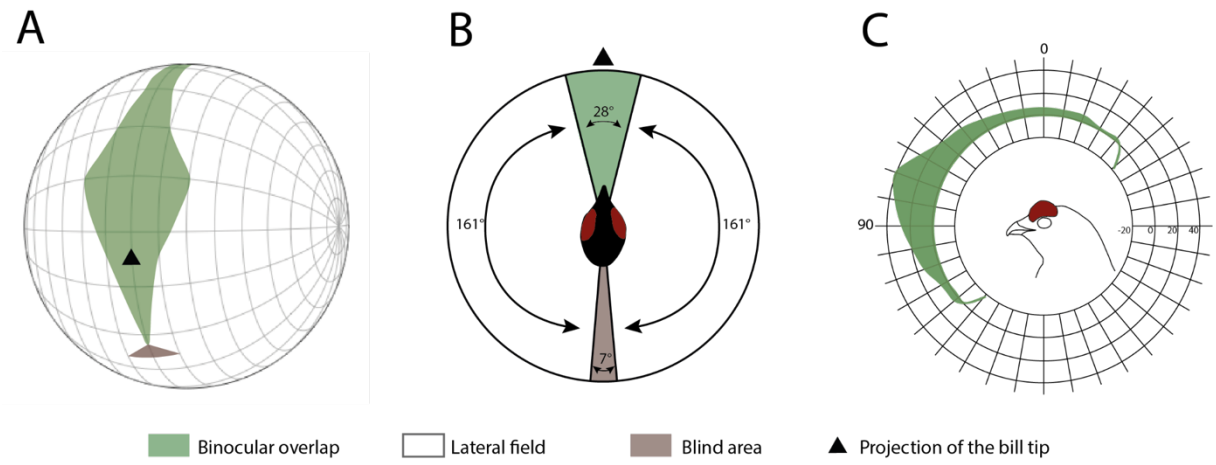

Figure 1: Visual fields of the black grouse. **(A)** Orthographic projection of the boundaries of the retinal fields of the two eyes. A latitude and longitude coordinate system was used with the equator aligned vertically in the median sagittal plane. The bird head is imagined to be at the centre of the globe with a grid at 20° intervals in latitude and 10° intervals in longitude. **(B)** Horizontal section through the horizontal plane (90-270°). **(C)** Binocular field as a function of elevation in the median sagittal plane. Orientation of the bird head is shown diagrammatically. All values are in degrees and the grid is at 10° intervals. Each chart represents the average retinal visual field when the eyes were converged. Green areas represent the binocular sector, white areas the monocular sectors and brown areas the blind sectors.

(b) Contrast sensitivity and visual acuity

Contrast sensitivity is dependent on the spatial resolution of the stimulus and is expressed as the inverse of Michelson contrast. We found a maximum contrast sensitivity of 16.67 for both individuals at a spatial frequency of 1.06 c/deg (Figure 2). Individual B had a similar contrast sensitivity value at 0.85 c/deg as well. This sensitivity corresponds to Michelson contrast of

6%. The extrapolated spatial resolution at highest contrast (contrast sensitivity = 1) was around 1.6 c/deg.

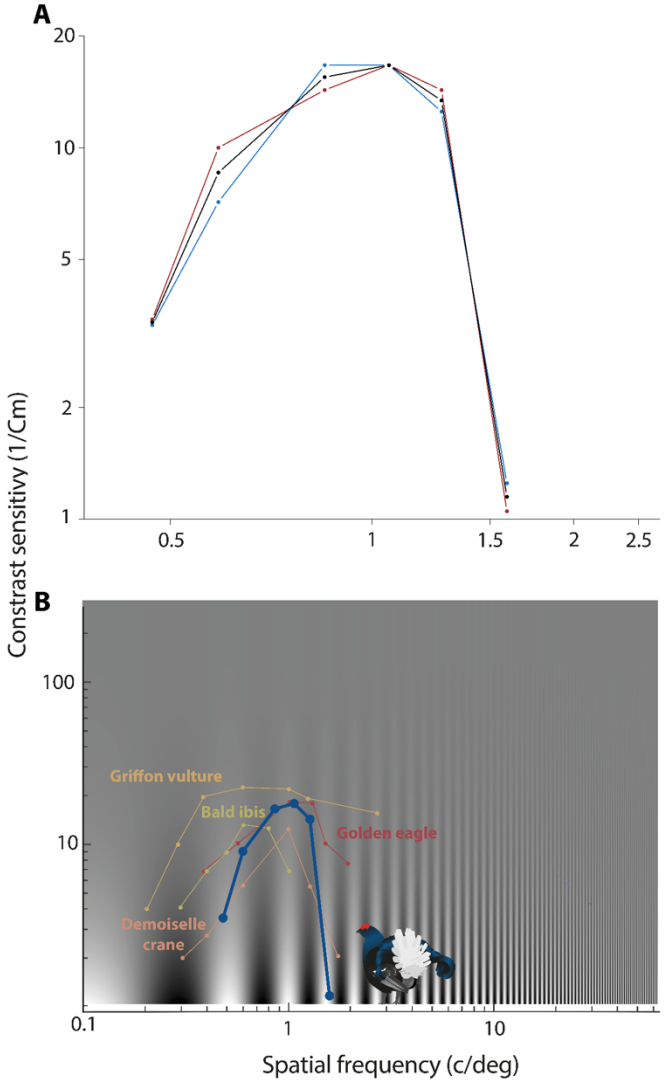

Figure 2: **Contrast sensitivity of the black grouse, defined as the inverse of contrast threshold, as a function of spatial frequency. (A)** Colored curves are individual values, black curve the pooled data. Note that the scales of the axes are logarithmic. **(B)** Comparison of the contrast sensitivity of the black grouse (blue) and selected species sensitive to collision.

The measured Corneal Diameter (CD) from close-up photographs was 8.00 mm for both individuals. The estimated Axial Length (AL) was therefore 13.28 mm, which corresponds to a spatial resolution of 9.81 c/deg.

(c) opsin spectral sensitivity

To determine the spectral sensitivity of cone opsins expressed in retinal photoreceptors of the black grouse, we first carried out a transcriptomic profiling to identify opsins mRNAs expressed and phylogenetic placement (SI data_Opsin Sequences) revealing 4 transcripts corresponding to known classes of bird visual cone opsins belonging to the short wavelength (SWS1 and SWS2), medium wavelength (MW or Rh2), and long wavelength (LW) subfamilies, as well as the dim-light sensitive rod opsin (Rh1) associated with achromatic rod vision.

Open reading frame sequences for cone opsins were subcloned into a modified pcDNA5-FLAG-T2A-mruby2 expression cassette and the resulting plasmid construct was transiently expressed in HEK293T cells. Active rhodopsin complexes were reconstituted in vitro by addition of *11*,cis-retinal, after which rhodopsin proteins were isolated from cell membranes and purified using FLAG resin affinity binding following Liénard et al. (2022). Concentrated rhodopsin eluates were analysed by ultraviolet-visible spectroscopy to determine the absorbance profiles of each opsin type. These analyses showed that the black grouse SWS1 and SWS2 opsins absorb maximally at λ_{max} of 393 ± 2nm (Figure 3A), and λ_{max} of 436 ± 3nm (Figure 3B). We then measured the absorbance of black grouse Rh2 and LW, which displayed maximum sensitivity to light at 482 nm ± 2.5 nm (Figure 3C) and 545 ± 2.5 nm (Figure 3D), respectively.

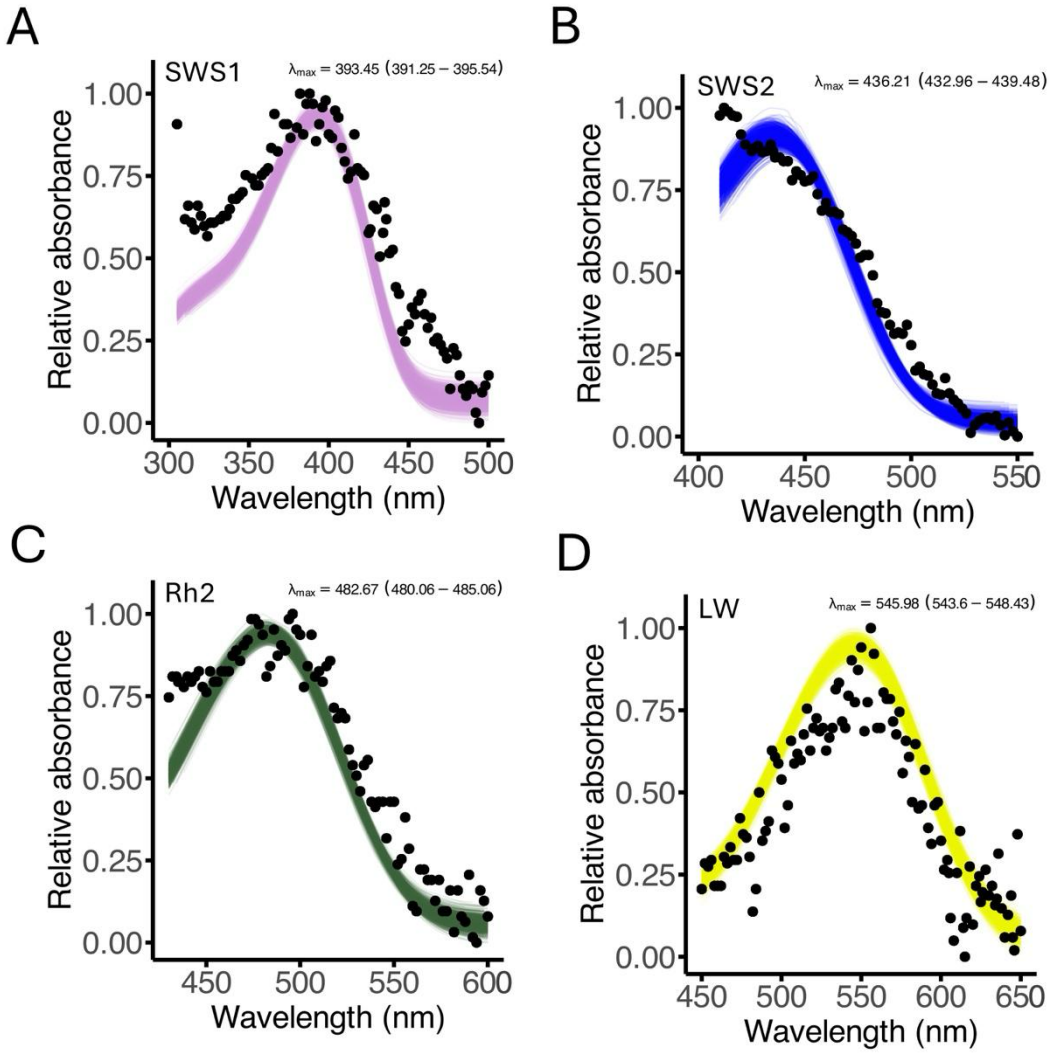

Figure 3: Functional expression of *Lyrurus tetrix* visual opsins. Absorbance curves **(A-D)** of visual rhodopsins reconstituted in presence of 11,*cis*-retinal and purified from HEK293T cells. The black dots represent the mean absorbance at every wavelength. **(A)** SW1 (n = 7), **(B)** SW2 (n = 6), **(C)** Rh2 (n = 3), **(D)** LW (n = 7), where n is the number of measurements of protein aliquots with active rhodopsin complexes. Relative absorbance data are fitted to a visual template with polynomial function analyses computed in R to obtain the best estimates following 1000 bootstrap analysis of lambda max for each rhodopsin (Liénard et al., 2022). Confidence intervals are indicated in parentheses. Accompanying data are provided in SI dataset 1.

Overall, the four visual opsins confer broad wavelength sensitivity from 300 to 650 nm (Figure 4A). Based on the measured spectral sensitivity of SWS1, we calculated the predicted theoretical cut-off value of C-type oil droplets in SWS2 cones following Hart (2001), which falls at approximately 430 nm (Table S3 – predicted cut-off C-type droplets; Figure 4B).

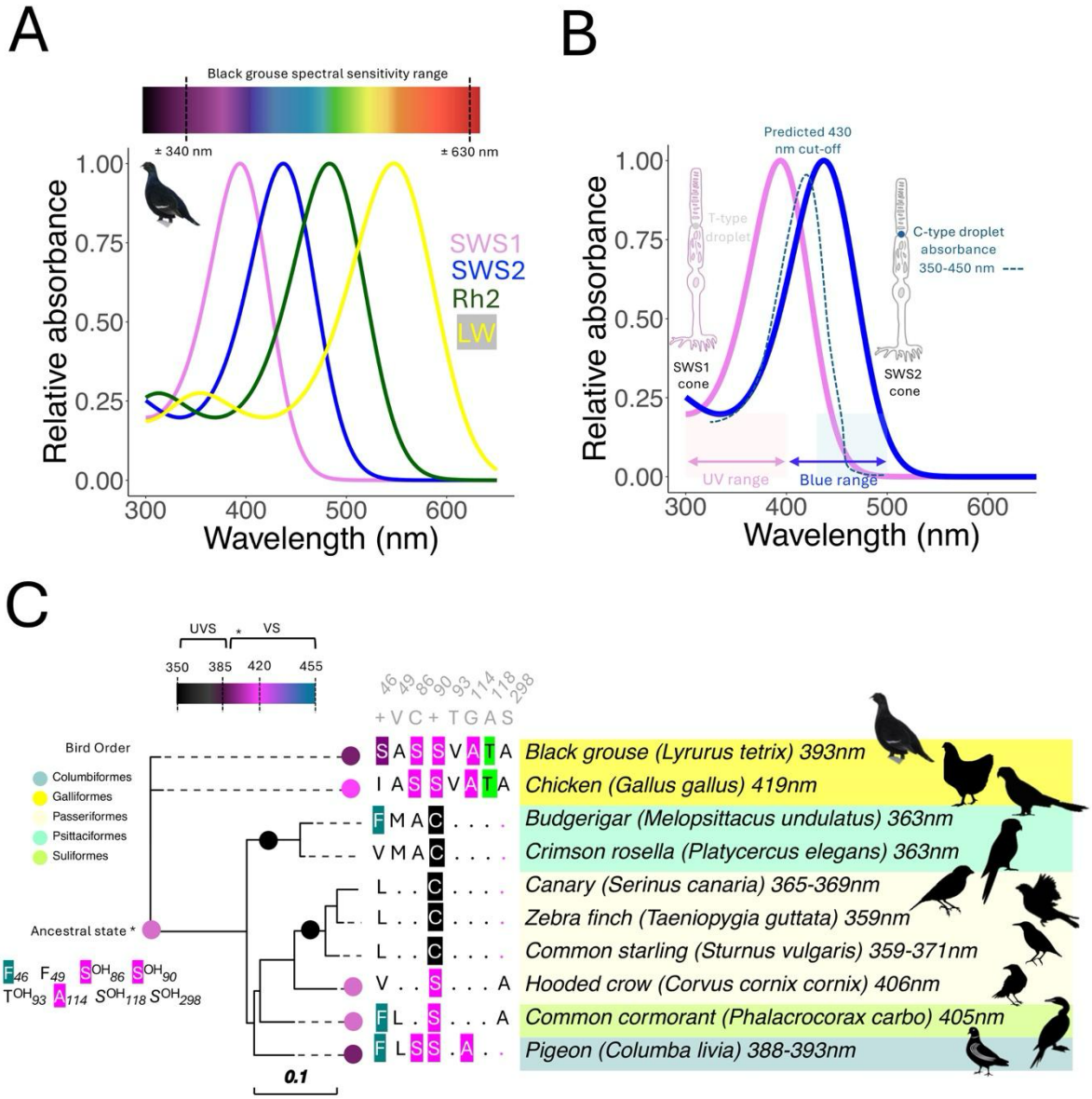

Figure 4: **Opsin spectral sensitivity curves in the Blackgrouse, *Lyrurus tetrix* and ultraviolet light perception**. **(A)** Spectral sensitivity curves for SWS1, SWS2, Rh2 and LW visual cone opsins confer broad light perception in the range 340 to 630 nm. **(B)** The presence of C-type droplets in bird SWS2 cones affects the perception of ultraviolet light, and a cut-off value can be predicted based on the maximal sensitivity of the SWS1 opsin (Table S4) (Hart, 2001), which for *Lyrurus tetrix* would be projected at 430 nm, indicating that the SWS2 cone would not absorb wavelengths shorter than 430 nm (dashed blue line). The SWS1 cones have transparent T-type oil droplets that do not absorb light, and the SWS1 cone would absorb near-UV light. **(C)** SWS1 opsin phylogeny of selected bird species with SWS1 opsin lambda max determined experimentally. Amino acid residue position known to be important for SWS1 maximal sensitivity. OH refers to amino acids bearing a hydroxyl group. Dots in the alignment correspond to the residue in the consensus sequence (in grey). The asterisk positions SWS1 as a near-UV sensitive pigment in the black grouse.

Discussion

The visual system of the black grouse indicates a relatively low spatial resolution and contrast sensitivity but a high visual coverage

The black grouse showed a high visual coverage but relatively low contrast sensitivity and visual acuity, visual characteristics that are typical from other prey species (Martin, 2017).
In birds, binocularity is thought to function primarily in the detection of symmetrically expanding optic flow-fields that provide almost instantaneous information on the direction of travel and time-to-contact a target (Martin, 2009, Martin & Portugal, 2011). The maximum width of the frontal binocular field was 28° and fell well within the range of other birds (20-40° on average) (Martin, 2017). Maximum binocular field width was found to be 30° below the eye bill-tip direction, similarly to other species that forage on the ground by vision such as the Southern caracara *Caracara plancus* (Potier et al., 2017). Therefore, it seems very likely that the binocular field of the black grouse represents an adaptation to its foraging technique, as found in many bird species (Martin & Portugal, 2011, Potier et al., 2018b, Potier et al., 2023).

The results on the visual field configuration of the black grouse also showed that this species has an exceptionally extended visual field (both on the horizontal and vertical plane). To date, on more than 150 species studied, only 4 species had a smaller blind spot behind the head (3 ducks: the Mallard *Anas platyrhynchos*, the Northern pintail *Anas acuta* and the Pink-eared duck *Malacorhynchus membranaceus*) (Martin, 1986, Guillemain & Fritz, 2002, Martin, 2007), as well as the Eurasian woodcock *Scolopax rusticola* (Martin, 1994). This configuration allows the black grouse to gain a comprehensive visual coverage of the celestial hemisphere. Black grouse adopting the typical head position depicted in Figure 2 can thus gather visual information from above the head without the need of head movements. This would allow foraging and predator detection to be conducted almost together.

While eye size correlates with visual field parameters in birds, such as blind spot above the head (Martin, 2007), larger eyes also confer higher visual acuity (Kiltie, 2000, Caves et al., 2024). The estimated visual acuity of the black grouse is relatively low compared to predatory species but similar to most prey species (Martin, 2017, Caves et al., 2024). Furthermore, our estimation of visual acuity based on eye size is very similar to closely related species from the same order Galliformes (based on 7 species, ranging from 9.7 c/deg for the Japanese quail *Coturnix japonica* to 13 c/deg for the Sharp-tailed grouse *Tympanuchus phasianellus* (Lisney et al., 2012). In terms of foraging, high visual acuity is not necessary while foraging on the

ground (Potier et al., 2016a), therefore, black grouse would not need to gain from having higher spatial resolving power of the eyes.

Finally, the maximum contrast sensitivity of the black grouse (16.67) is similar to other birds tested so far, ranging from 4.8 for the Bourke's parrot *Neopsephotus bourkii* to 31 for the American kestrel *Falco sparverius* (Hirsch, 1982, Lind et al., 2012, Blary et al., 2024). The contrast sensitivity of the black grouse is therefore 4.5 to 10.5 times lower than large mammals (Bisti & Maffei, 1974, De Valois et al., 1974, Merigan, 1976, Jacobs, 1977, Langston et al., 1986) but similar to small mammals such as rats (Birch & Jacobs, 1979, Keller et al., 2000). It is not fully understood why birds have relatively low contrast sensitivity. One possible reason could be a trade-off between contrast and color sensitivity (Ghim & Hodos, 2006). Indeed, most birds perceive more colors than the majority of mammals (Hart, 2001), and some can perceive colors at greater distances (Potier et al., 2018a). In black grouse, the presence of a fourth type of cone sensitive to very short wavelengths near the ultraviolet region may be potentially energetically costly (Niven & Laughlin, 2008). Hence, in mammals, species sensitive to UV light, such as rats, have lower contrast sensitivity than species that are non-sensitive to UV light, such as primates (De Valois et al., 1974, Merigan, 1976, Jacobs, 1977, Birch & Jacobs, 1979, Langston et al., 1986, Keller et al., 2000, Hunt et al., 2001).

Opsin-based visual spectral sensitivity confers broad wavelength perception and presumably near-ultraviolet vision

There has been a long-standing interest in determining the possible role of ultraviolet light and spectral sensitivities at short wavelengths in animal vision, in the context of intra- and inter-specific signalling but also foraging abilities across animal groups, including in invertebrates (Cronin & Bok, 2016, McCulloch et al., 2017, Finkbeiner & Briscoe, 2021); terrestrial vertebrates including snakes (Crowell et al., 2024), lizards (Pérez i de Lanuza & Font, 2014) and birds (Massaro et al., 2003).

In particular, avian and mammalian SWS1 visual pigments exhibit a broad natural variation from very short UV sensitivity to violet sensitivity and have been studied at the molecular and *in silico* level in relatively great details (Hunt et al., 2009, Hauser et al., 2014, Yokoyama et al., 2016, Patel et al., 2018). The four cone opsins (SWS1, SWS2, Rh2 and LW) characterized from the Black grouse retina and reconstituted *in vitro* via heterologous expression showed maximal peak sensitivities at 393 nm (SWS1), 436 nm (SWS2), 482 nm (Rh2), and 546 nm (LW) (Figure 3). Our results align with observed spectral ranges across bird

species investigated to date (reviewed in Hauser et al., 2014, Hagen et al., 2023), supporting that opsin-based spectral sensitivity confers light perception from ultraviolet (UV) wavelengths to very long wavelength light, from 340 to 650 nm (Figure 4).

The 393 nm sensitivity of black grouse SWS1 is an interesting intermediate between known very shifted UV sensitive, and violet SWS1 bird pigments (Figure 4C). Several spectral tuning sites have been identified that contribute to expand the absorbance of SWS1 opsins from violet to shorter ultraviolet light (Figure 4C) (e.g. Hagen et al., 2023). In particular, ancestrally, birds most likely possessed a violet-sensitive SWS1 pigment, whereas ultraviolet sensitivity has been regained subsequently in certain lineages (Shi et al., 2001), allowing visual and ecological adaptations (Hauser & Chang, 2017, Hauser et al., 2014, Hagen et al., 2023). Also, the variability of avian SWS1 spectral tuning residues seems overall more consistent than residues regulating mammalian and other vertebrate SWS1 pigment sensitivity (Hauser et al., 2014), which can be explained to a large degree by amino acid convergence at specific sites (Figure 4C) (Hauser et al., 2014). Yet, it remains interesting to obtain more experimental *in vitro* expression data on additional SWS1 opsins, to further improve evolutionary inferences of extant UV-violet spectral sensitivity across the entire avian class. The galliform blackgrouse, although phylogenetically related to the chicken *Gallus gallus*, has its SWS1 pigment absorb in the near-UV (393 nm) similarly to the distantly related Columbiform pigeon *Columba liva* SWS1 pigment (Figure 4C) (Bowmaker, 1977). Although it is possible that small differences in measured spectral sensitivities for pigments purified *in vitro* may account for variations in experimental methods, several bird SWS1 have been shown previously to confer near-UV vision owing to measured properties of SWS1 pigments themselves, or *in silico* sequence predictions (Carvalho et al., 2007a, Hauser et al., 2014). The black grouse exhibits many conserved spectral tuning sites of SWS1 with its close orthologue in the chicken yet exhibits a Serine residue at spectral tuning position 46 (Ser46), which may play a role in intermediate spectral sensitivity.

In birds, the ocular media are often UV transparent, especially for birds with UV-sensitive visual pigments (Lind et al., 2014), making sensitivity to UV wavelengths possible in cones expressing an ultraviolet-sensitive SWS1 visual pigment (reviewed in Cuthill et al., 2000). Colour vision in bird visual cones is however affected by distinct types of oil droplets that filter incoming light in the bird retina (Kelber, 2019). Cone oil droplets are positioned between incoming light and the cone visual pigments, acting as a filter which can influence the pigment's effective spectral sensitivity by absorbing part of the incoming light spectrum. The

oil droplet type in SWS1 cones is transparent (Hart, 2001) and leaves the opsin pigment intrinsic sensitivity. In SWS2 cones, the cone peak sensitivity is typically shifted to a wavelength longer than the opsin pigment inherent lambda max (Bowmaker, 1977, Olsson et al., 2017). This effect can be predicted based on SWS1 lambda max (Hart, 2001), overall reducing spectral sensitivity of SWS2 below 400 nm (Figure 4). Overall, oil droplets will thus reduce chromatic abilities while maintaining sensitivity to UV wavelengths (achromatic vision), owing to the black grouse SWS1 pigment function.

The behavioural role of UV vision in foraging has also been demonstrated. If some UV wavelengths are present in the light environment, several bird species exhibit enhanced detection of UV reflecting food items. For instance, Church et al. (1998) showed that blue tits' foraging ability is enhanced by UV cues of cryptic caterpillars. Behavioural experiments showed the ability for several bird species, including redwing *Turdus iliacus* (Siitari et al., 2002) and black grouse (Siitari et al., 2002) to discriminate UV wavelengths. Black grouse show a preference for European blueberries (*Vaccinium myrtillus*) reflecting UV owing to their natural wax coat compared to non-UV reflecting fruits (Siitari et al., 2002). Even if some part of the UV spectrum is likely filtered out due to typical oil droplets in bird SWS2 cones, not allowing true UV colour vision, black grouse still detect UV wavelengths and are sensitive even to low ultraviolet light intensities. Together, behavioural evidence with our opsin-based absorbance spectra results strongly support UV sensitivity in this species.

Recapitulating visual properties to inform vision-based collision mitigation

Birds' visual capabilities has been hypothesised as a major cause of collision with man-made objects (Martin, 2011a, Martin, 2022, Martin & Banks, 2023). However, vision is a complex and multifaceted sense, underlying the necessity to explore different visual characteristics. In this study, we had an integrative approach by exploring black grouse visual fields, contrast sensitivity, eye size (and therefore visual acuity) and spectral sensitivity. All these visual capacities have been listed as essential in the context of collision, in addition to speed of vision (Martin, 2022).

For instance, many birds fail to see the way ahead, such as large raptors from Accipitriformes (Martin et al., 2012, Portugal et al., 2017, Potier et al., 2018b). Indeed, while searching the ground below for food, those raptors would gain no or intermittent information about the flight path ahead (Martin et al., 2012). This is especially true in familiar open habitats, and when an unpredictable change occurs, such as human artefacts, that may lead to fatal

collisions (Martin, 2022). We find that black grouse have an extended visual coverage, conferring them the ability to see the way ahead. Therefore, its visual field configuration itself, should allow it to gather environmental information, such as the presence of an aerial object. This is interesting because it opens opportunities to optimize the visual perception of man-made objects by modifying the contrast (within the object or compare to the background), colours, or using bird diverters for instance (Martin, 2022) to reduce the high number of collisions in this species.

In contrast, Black grouse would have a relatively low spatial resolving power (9.81 c/deg), which tells us how far it can see in optimal conditions, including i) no air distortion and clear sky, ii) black object on a white background, iii) high daytime level, iv) the bird visually fixing the object with its acute centre of vision (Land & Nilsson, 2012, Martin, 2017, Martin, 2022). In this case, the distance at which an object is detectable and avoidable depends on i) the spatial resolving power, ii) the time to process the information and iii) the flight speed. In birds, it is reasonable to assume a requirement of at least 2 seconds to take the action of changing flight path (Martin, 2022), although this prediction has to be confirmed by species-specific experimental validation. The flight speed of black grouses can be deduced according to a clear existing relationship between body mass (1068.7g for the black grouse (Dunning, 2007)) and flight speed 16.04 m.s-1 (35.88 mph), derived from Alerstam et al. (2007). Therefore, giving a minimal estimated detection time of 2 sec, the shortest distance at which the black grouse can detect and avoid an object is 32m. According to the estimated visual acuity, trigonometric calculations indicate that this object should be of a minimum size of 50mm^2. However, in a natural scene, optimal conditions are barely reached. Spatial resolution declines significantly with light level (Land & Nilsson, 2012), and a 5-fold decrease from maximum spatial resolution should be highly likely (Martin, 2022). In this case, the object should be 5 times bigger, therefore of a minimum size of 250mm^2. Because black grouse maximum contrast sensitivity, similarly to other birds, is relatively low, the internal object contrast, as well as the contrast between the object and its surrounding environment should be as high as possible (Martin, 2022). Also, under natural conditions, the range of background conditions against which an object appears is highly variable, and maximising internal object contrast should be privileged.

Finally, spectral and achromatic sensitivity may play an additional role in object detection. Arguably, colors are typically detectable only at high light levels and should not be used to generate contrast patterns alone (Land & Nilsson, 2012), also because the chromatic spatial resolution is generally lower than the achromatic one in birds (Lind & Kelber, 2011, Potier et al., 2018a). However, our results indicated that black grouses have an intermediate

near-UV-sensitive type of SWS1 cone, similarly to SWS1 cones in the pigeon *Columba livia* (Carvalho et al., 2007a). Because the oil droplets present in bird SWS1 photoreceptors are mainly transparent (Hart, 2001), black grouse perceive these short-wavelengths of light, which might open avenues to implement diverters reflecting UV or near-UV wavelengths imperceptible by humans. For instance, the use of UV lamps actively emitting short wavelengths (380-390 nm) on power poles has been shown to reduce night collisions of Sandhill Cranes *Grus canadensis* with power lines by 98% (Dwyer et al., 2019). Incorporating the use of natural surfaces reflecting short wavelengths in collision diverter design may be a promising avenue contributing to reducing bird collisions with man-made objects (Baasch et al., 2022). Therefore, although colour vision in the short-wavelength range is likely restricted to a narrower spectrum, due to characteristics of the cornea and lens, including the presence of filtering oil droplets in SWS2 cones, if diverters are used to reduce black grouse collisions, a UV reflection would be beneficial. The reflectance properties of detection materials implemented in natural conditions were measured to gain a better understanding of the emission spectrum of diffuse and specular light rays (See supplementary materials). By comparing a large diversity of diverters currently used to date in french Alps ski areas, we found that most reflect visible wavelengths of light, but none of them reflect wavelengths shorter than 400 nm (UV range) while some diverters already had good internal contrasts, suggesting that with little modification, such as increased size, improved contrast and short-wavelength reflective-material, diverters would allow a better aerial cable detection by black grouses which may contribute to a significant reduction of collisions.

Ethics

Ethical approval for the handling and restraint of birds was granted under the permit number APAFIS# 31775-31775-2021041311196892 v5. Permissions were granted from the owner of the birds used in the study.

Data accessibility

All data are available as electronic supplementary material.

Conflict of interest declaration

The authors declare no competing interests.

Funding

This study was funded by the Parc National de la Vanoise, and by grants from the Swedish Research Council (2020-05107) and the Belgian F.R.S/FNRS (MISU F.6002.24) to MAL. J.M.L is supported by a MISU grant from the FRS-FNRS (F.6002.22).

Acknowledgements

We are extremely grateful to Frank Grosemans for access to its birds, to Dr. Pascal Barla for its expertise on spectral rays, and to FDC38 for access to eye tissue material. The computations in this paper were run on the GIGA Cluster at ULiège.

References

Aidala, Z., Huynen, L., Brennan, P. L., Musser, J., Fidler, A., Chong, N., Machovsky Capuska, G. E., Anderson, M. G., Talaba, A., Lambert, D. & Hauber, M. E. 2012. Ultraviolet visual sensitivity in three avian lineages: paleognaths, parrots, and passerines. *J Comp Physiol A Neuroethol Sens Neural Behav Physiol* **198**: 495-510.

Alerstam, T., Rosén, M., Bäckman, J., Ericson, P. G. P. & Hellgren, O. 2007. Flight Speeds among Bird Species: Allometric and Phylogenetic Effects. *PLOS Biology* **5**: e197.

Baasch, D. M., Caven, A. J., Jorgensen, J. G., Grosse, R., Rabbe, M., Varner, D. M. & LaGrange, T. 2022. Whooping Crane (Grus americana) use patterns in relation to an ecotope classification in the Central Platte River Valley, Nebraska, USA. *Avian Conservation and Ecology* **17**.

Bech, N., Beltran, S., Boissier, J., Allienne, J., Resseguier, J. & Novoa, C. 2012. Bird mortality related to collisions with ski-lift cables: do we estimate just the tip of the iceberg?. *Animal Biodiversity and Conservation* **35**: 95-98.

Bernardino, J., Bevanger, K., Barrientos, R., Dwyer, J. F., Marques, A. T., Martins, R. C., Shaw, J. M., Silva, J. P. & Moreira, F. 2018. Bird collisions with power lines: State of the art and priority areas for research. *Biological Conservation* **222**: 1-13.

Birch, D. & Jacobs, G. H. 1979. Spatial contrast sensitivity in albino and pigmented rats. *Vision Res* **19**: 933-7.

Bisti, S. & Maffei, L. 1974. Behavioural contrast sensitivity of the cat in various visual meridians. *J Physiol* **241**: 201-10.

Blary, C. L. M., Duriez, O., Bonadonna, F., Mitkus, M., Caro, S. P., Besnard, A. & Potier, S. 2024. Low achromatic contrast sensitivity in birds: a common attribute shared by many phylogenetic orders. *J Exp Biol* **227**.

Borges, R., Khan, I., Johnson, W. E., Gilbert, M. T. P., Zhang, G., Jarvis, E. D., O'Brien, S. J. & Antunes, A. 2015. Gene loss, adaptive evolution and the co-evolution of plumage coloration genes with opsins in birds. *BMC Genomics* **16**: 751.

Bowmaker, J. K. 1977. The visual pigments, oil droplets and spectral sensitivity of the pigeon. *Vision Research* **17**: 1129-1138.

Brainard, D. H. 1997. The Psychophysics Toolbox. *Spat Vis* **10**: 433-6.

Brooke, M., Hanley, S. & Laughlin, S. 1999. The scaling of eye size with body mass in birds. *Proc Biol Sci* **266**: 405.

Bryant, D. M., Johnson, K., Tia, D., Tickle, T., Couger, M. B., Payzin-Dogru, D., Lee, T., Leigh, N., Kuo, T., . & Whited, J. 2017. A Tissue-Mapped Axolotl De Novo Transcriptome Enables Identification of Limb Regeneration Factors. *Cell rep* **18**: 762-776.

Buffet, N. & Dumont-Dayot, E. (2013) Bird collisions with overhead ski-cables: a reducible source of mortality. In: *The Impacts of Skiing and Related Winter Recreational Activities on Mountain Environments.* pp. 123-136. Eureka select.

Cantlay, J. C., Martin, G. R., McClelland, S. C., Potier, S., O'Brien, M. F., Fernández-Juricic, E., Bond, A. L. & Portugal, S. J. 2023. Binocular vision and foraging in ducks, geese and swans (Anatidae). *Proceedings of the Royal Society B: Biological Sciences* **290**: 20231213.

Carvalho, L., Cowing, J., Wilkie, S. & Hunt, D. 2007a. The molecular evolution of avian ultraviolet- and violet-sensitive visual pigments. *Mol Biol Evol* **24**: 1843-1852.

Carvalho, L. S., Cowing, J. A., Wilkie, S. E., Bowmaker, J. K. & Hunt, D. M. 2007b. The molecular evolution of avian ultraviolet- and violet-sensitive visual pigments. *Mol Biol Evol* **24**: 1843-52.

Carvalho, L. S., Knott, B., Berg, M. L., Bennett, A. T. D. & Hunt, D. M. 2011. Ultraviolet-sensitive vision in long-lived birds. *Proceedings of the Royal Society B: Biological Sciences* **278**: 107-114.

Caves, E. M., Fernández-Juricic, E. & Kelley, L. A. 2024. Ecological and morphological correlates of visual acuity in birds. *J Exp Biol* **227**.

Church, S. C., Bennett, A. T. D., Cuthill, I. C. & Partridge, J. C. 1998. Ultraviolet cues affect the foraging behaviour of blue tits. *Proceedings of the Royal Society of London. Series B: Biological Sciences* **265**: 1509-1514.

Cooney, C. R., Varley, Z. K., Nouri, L. O., Moody, C. J. A., Jardine, M. D. & Thomas, G. H. 2019. Sexual selection predicts the rate and direction of colour divergence in a large avian radiation. *Nat Commun* **10**: 1773.

Corredor, V. H., Hauzman, E., Gonçalves, A. d. S. & Ventura, D. F. 2022. Genetic characterization of the visual pigments of the red-eared turtle (Trachemys scripta elegans) and computational predictions of the spectral sensitivity. *Journal of Photochemistry and Photobiology* **12**: 100141.

Cronin, T. W. & Bok, M. J. 2016. Photoreception and vision in the ultraviolet. *Journal of Experimental Biology* **219**: 2790-2801.

Crowell, H. L., Curlis, J. D., Weller, H. I. & Davis Rabosky, A. R. 2024. Ecological drivers of ultraviolet colour evolution in snakes. *Nature Communications* **15**: 5213.

Cuthill, I. C., Partridge, J. C., Bennett, A. T. D., Church, S. C., Hart, N. S. & Hunt, S. (2000) Ultraviolet Vision in Birds. In: *Advances in the Study of Behavior*, Vol. 29 (Slater, P. J. B., Rosenblatt, J. S., Snowdon, C. T. & Roper, T. J., eds.). pp. 159-214. Academic Press.

De Valois, R. L., Morgan, H. & Snodderly, D. M. 1974. Psychophysical studies of monkey Vision-III. Spatial luminance contrast sensitivity tests of macaque and human observers. *Vision Research* **14**: 75-81.

Dunning, J. 2007. *CRC Handbook of Avian Body Masses*. Boca Raton.

Dwyer, J., Pandey, A., McHale, L. & Harness, H. 2019. Near-ultraviolet light reduced Sandhill Crane collisions with a power line by 98%. *The Condor*: 1-10.

Fernandez-juricic, E., Gall, M., Dolan, T., Tisdale, V. & Martin, G. 2008. The visual fields of two ground-foraging birds, House Finches and House Sparrows, allow for simultaneous foraging and anti-predator vigilance. *Ibis* **150**: 779-787.

Ferrer, M., Morandini, V., Baumbusch, R., Muriel, R., De Lucas, M. & Calabuig, C. 2020. Efficacy of different types of "bird flight diverter" in reducing bird mortality due to collision with transmission power lines. *Global Ecology and Conservation* **23**: e01130.

Finkbeiner, S. D. & Briscoe, A. D. 2021. True UV color vision in a female butterfly with two UV opsins. *J Exp Biol* **224**.

Frentiu, F. D. & Briscoe, A. D. 2008. A butterfly eye's view of birds. *BioEssays* **30**: 1151-1162.

Frick, H., Chow, F., Kuhn, M., Mahoney, M., Silge, J. & Wickham, H. (2022) Rsample: General Resampling Infrastructure. R package version 1.1.1. pp.

Ghim, M. M. & Hodos, W. 2006. Spatial contrast sensitivity of birds. *J Comp Physiol A Neuroethol Sens Neural Behav Physiol* **192**: 523-34.

Goldsmith, T. H. 1990. Optimization, Constraint, and History in the Evolution of Eyes. *The Quarterly Review of Biology* **65**: 281-322.

Govardovskii, V., Fyhrquist, N., Reuter, T., Kuzmin, D. & Donner, K. 2000. In search of the visual pigment template. *Vis Neurosci* **17**: 509-528.

Grabherr, M. G., Haas, B. J., Yassour, M., Levin, J. Z., Thompson, D. A., Amit, I., Adiconis, X., Fan, L., Raychowdhury, R., Zeng, Q., Chen, Z., Mauceli, E., Hacohen, N., Gnirke, A., Rhind, N., di Palma, F., Birren, B. W., Nusbaum, C., Lindblad-Toh, K., Friedman, N. & Regev, A. 2011. Full-length transcriptome assembly from RNA-Seq data without a reference genome. *Nature Biotechnology* **29**: 644.

Guillemain, M. & Fritz, H. 2002. Temporal variation in feeding tactics: exploring the role of competition and predators in wintering dabbling ducks. *Wildlife Biology* **8**: 81-90, 10.
Hagen, J. F. D., Roberts, N. S. & Johnston, R. J. 2023. The evolutionary history and spectral tuning of vertebrate visual opsins. *Developmental Biology* **493**: 40-66.
Hall, M. I. & Ross, C. F. 2007. Eye shape and activity pattern in birds. *Journal of Zoology* **271**: 437-444.
Hart, N. S. 2001. The visual ecology of avian photoreceptors. *Prog Retin Eye Res* **20**: 675-703.
Hart, N. S. & Hunt, D. M. 2007. Avian visual pigments: characteristics, spectral tuning, and evolution. *Am Nat* **169 Suppl 1**: S7-26.
Hauser, F. & Chang, B. 2017. Insights into visual pigment adaptation and diversity from model ecological and evolutionary systems. *Current opinion in genetics & development* **47**: 110-120.
Hauser, F. E., Hazel, I. v. & Chang, B. S. W. 2014. Spectral tuning in vertebrate short wavelength-sensitive 1 (SWS1) visual pigments: Can wavelength sensitivity be inferred from sequence data? *J Exp Zool* **322**: 529-539.
Hirsch, J. 1982. Falcon visual sensitivity to grating contrast. *Nature* **300**: 57-58.
Hunt, D. M., Carvalho, L. S., Cowing, J. A. & Davies, W. L. 2009. Evolution and spectral tuning of visual pigments in birds and mammals. *Philos Trans R Soc Lond B Biol Sci* **364**: 2941-55.
Hunt, D. M., Carvalho, L. S., Cowing, J. A., Parry, J. W., Wilkie, S. E., Davies, W. L. & Bowmaker, J. K. 2007. Spectral tuning of shortwave-sensitive visual pigments in vertebrates. *Photochem Photobiol* **83**: 303-10.
Hunt, D. M., Wilkie, S. E., Bowmaker, J. K. & Poopalasundaram, S. 2001. Vision in the ultraviolet. *Cell Mol Life Sci* **58**: 1583-98.
Jacobs, G. 1977. Visual capacities of the owl monkey (*Aotus trivirgatus*): II. Spatial contrast sensitivity. *Vision Res* **17**: 821-825.
Kelber, A. 2019. Bird colour vision - from cones to perception. *Current opinion in Behavioral Sciences* **30**: 34-40.
Keller, J., Strasburger, H., Cerutti, D. T. & Sabel, B. A. 2000. Assessing spatial vision - automated measurement of the contrast-sensitivity function in the hooded rat. *J Neurosci Methods* **97**: 103-10.
Kiltie, R. A. 2000. Scaling of visual acuity with body size in mammals and birds. *Functional Ecology* **14**: 226-234.
Knott, B., Berg, M. L., Morgan, E. R., Buchanan, K. L., Bowmaker, J. K. & Bennett, A. T. 2010. Avian retinal oil droplets: dietary manipulation of colour vision? *Proc Biol Sci* **277**: 953-62.
Kuhn, M. & Wickham, H. (2020) Tidymodels: a collection of packages for modeling and machine learning using tidyverse principles. . pp.
Land, M. F. & Nilsson, D. E. 2012. *Animal eyes*. OUP Oxford, Oxford
Langmead, B. & Salzberg, S. L. 2012. Fast gapped-read alignment with Bowtie 2. *Nat Methods* **9**: 357-9.
Langston, A., Casagrande, V. A. & Fox, R. 1986. Spatial resolution of the galago. *Vision Research* **26**: 791-796.
Laughlin, S. B., de Ruyter van Steveninck, R. R. & Anderson, J. C. 1998. The metabolic cost of neural information. *Nat Neurosci* **1**: 36-41.
Li, B. & Dewey, C. N. 2011. RSEM: accurate transcript quantification from RNA-Seq data with or without a reference genome. *BMC Bioinformatics* **12**: 323.
Liénard, M., Bernard, G. D., Allen, A., Lassance, J., Song, S., Childers, R., Yu, N., Ye, D., Stephenson, A., Valencia-Montoya, W., Salzman, S., Whitaker, M., Calonje M, Zhang,

F. & Pierce, N. 2021. The evolution of red colour vision is linked to coordinated rhodopsin tuning in lycaenid butterflies. *PNAS* **118** e2008986118.
Liénard, M. A., Valencia-Montoya, W. A. & Pierce, N. E. 2022. Molecular advances to study the function, evolution and spectral tuning of arthropod visual opsins. *Philosophical Transactions of the Royal Society B: Biological Sciences* **377**.
Lim, H. H. & Pike, T. W. 2016. Dietary carotenoid availability affects avian color discrimination. *Behavioral Ecology* **27**: 1579-1584.
Lind, O. & Kelber, A. 2011. The spatial tuning of achromatic and chromatic vision in budgerigars. *Journal of Vision* **11**: 2-2.
Lind, O., Mitkus, M., Olsson, P. & Kelber, A. 2014. Ultraviolet vision in birds: the importance of transparent eye media. *Proceedings of the Royal Society B: Biological Sciences* **281**: 20132209.
Lind, O., Sunesson, T., Mitkus, M. & Kelber, A. 2012. Luminance-dependence of spatial vision in budgerigars (Melopsittacus undulatus) and Bourke's parrots (Neopsephotus bourkii). *Journal of Comparative Physiology A* **198**: 69-77.
Lisney, T. J., Iwaniuk, A. N., Kolominsky, J., Bandet, M. V., Corfield, J. R. & Wylie, D. R. 2012. Interspecifc variation in eye shape and retinal topography in seven species of galliform bird (Aves: Galliformes: Phasianidae). *J Comp Physiol A Neuroethol Sens Neural Behav Physiol* **198**: 717-31.
Marques, A. T., Batalha, H., Rodrigues, S., Costa, H., Pereira, M. J. R., Fonseca, C., Mascarenhas, M. & Bernardino, J. 2014. Understanding bird collisions at wind farms: An updated review on the causes and possible mitigation strategies. *Biological Conservation* **179**: 40-52.
Martin, G. 2011a. Understanding bird collisions with man-made objects: a sensory ecology approach. *Ibis* **153**: 239-254.
Martin, G. 2017. *The sensory ecology of birds*. Oxford University Press.
Martin, G. & Portugal, S. 2011. Differences in foraging ecology determine variation in visual fields in ibises and spoonbills (Threskiornithidae). *Ibis* **153**: 662-671.
Martin, G., Portugal, S. & Murn, C. 2012. Visual fields, foraging and collision vulnerability in Gyps vultures. *Ibis* **154**: 626-631.
Martin, G. R. 1984. The visual fields of the tawny owl, Strix aluco L. *Vision Research* **24**: 1739-1751.
Martin, G. R. 1986. Total panoramic vision in the mallard duck, Anas platyrhynchos. *Vision Res* **26**: 1303-5.
Martin, G. R. 1994. Visual fields in woodcocks Scolopax rusticola (Scolopacidae; Charadriiformes). *Journal of Comparative Physiology A* **174**: 787-793.
Martin, G. R. 2007. Visual fields and their functions in birds. *Journal of Ornithology* **148**: 547-562.
Martin, G. R. 2009. What is binocular vision for? A birds' eye view. *Journal of Vision* **9**: 14-14.
Martin, G. R. 2014. The subtlety of simple eyes: the tuning of visual fields to perceptual challenges in birds. *Philos Trans R Soc Lond B Biol Sci* **369**: 20130040.
Martin, G. R. 2022. Vision-Based Design and Deployment Criteria for Power Line Bird Diverters. *Birds* **3**: 410-422.
Martin, G. R. & Banks, A. N. 2023. Marine birds: Vision-based wind turbine collision mitigation. *Global Ecology and Conservation* **42**: e02386.
Martin, M. 2011b. Cutadapt removes adapter sequences from high-throughput sequencing reads. *2011* **17**: 3.

Massaro, M., Davis, L. S. & Darby, J. T. 2003. Carotenoid-derived ornaments reflect parental quality in male and female yellow-eyed penguins (Megadyptes antipodes). *Behavioral Ecology and Sociobiology* **55**: 169-175.

McCulloch, K. J., Yuan, F., Zhen, Y., Aardema, M. L., Smith, G., Llorente-Bousquets, J., Andolfatto, P. & Briscoe, A. D. 2017. Sexual Dimorphism and Retinal Mosaic Diversification following the Evolution of a Violet Receptor in Butterflies. *Molecular Biology and Evolution* **34**: 2271-2284.

Merigan, W. 1976. The contrast sensitivity of the squirrel monkey (Saimiri sciureus). *Vision Research* **16**: 375-379.

Meyer, D. B. (1977) The Avian Eye and its Adaptations. pp.

Moore, B. A., Pita, D., Tyrrell, L. P. & Fernández-Juricic, E. 2015. Vision in avian emberizid foragers: maximizing both binocular vision and fronto-lateral visual acuity. *Journal of Experimental Biology* **218**: 1347-1358.

Moran, D., Softley, R. & Warrant, E. J. 2015. The energetic cost of vision and the evolution of eyeless Mexican cavefish. *Science Advances* **1**: e1500363.

Nachtigall, P. G., Grazziotin, F. G. & Junqueira-de-Azevedo, I. L. M. 2021. MITGARD: an automated pipeline for mitochondrial genome assembly in eukaryotic species using RNA-seq data. *Brief Bioinform* **22**.

Niven, J. E. & Laughlin, S. B. 2008. Energy limitation as a selective pressure on the evolution of sensory systems. *J Exp Biol* **211**: 1792-804.

O'Rourke, C. T., Hall, M. I., Pitlik, T. & Fernández-Juricic, E. 2010. Hawk Eyes I: Diurnal Raptors Differ in Visual Fields and Degree of Eye Movement. *PLOS ONE* **5**: e12802.

Odeen, A. & Håstad, O. 2010. Pollinating birds differ in spectral sensitivity. *J Comp Physiol A Neuroethol Sens Neural Behav Physiol* **196**: 91-6.

Olsson, P., Lind, O. & Kelber, A. 2017. Chromatic and achromatic vision: parameter choice and limitations for reliable model predictions. *Behavioral Ecology* **29**: 273-282.

Outomuro, D., Söderquist, L., Johansson, F., Ödeen, A. & Nordström, K. 2017. The price of looking sexy: visual ecology of a three-level predator–prey system. *Functional Ecology* **31**: 707-718.

Patel, J., Brown, C., Ytreberg, F. & Stenkamp, D. 2018. Predicting peak spectral sensitivities of vertebrate cone visual pigments using atomistic molecular simulations. *PLOS Computational Biology* **14**: e1005974.

Pérez i de Lanuza, G. & Font, E. 2014. Ultraviolet vision in lacertid lizards: evidence from retinal structure, eye transmittance, SWS1 visual pigment genes and behaviour. *J Exp Biol* **217**: 2899-909.

Portugal, S. J., Sivess, L., Martin, G. R., Butler, P. J. & White, C. R. 2017. Perch height predicts dominance rank in birds. *Ibis* **159**: 456-462.

Potier, S., Bonadonna, F., Kelber, A. & Duriez, O. 2016a. Visual acuity in an opportunistic raptor, the chimango caracara (Milvago chimango). *Physiol Behav* **157**: 125-8.

Potier, S., Bonadonna, F., Kelber, A., Martin, G. R., Isard, P.-F., Dulaurent, T. & Duriez, O. 2016b. Visual abilities in two raptors with different ecology. *Journal of Experimental Biology* **219**: 2639-2649.

Potier, S., Bonadonna, F., Martin, G. R., Isard, P.-F., Dulaurent, T., Mentek, M. & Duriez, O. 2018a. Visual configuration of two species of Falconidae with different foraging ecologies. *Ibis* **160**: 54-61.

Potier, S., Duriez, O., Cunningham, G. B., Bonhomme, V., O'Rourke, C., Fernández-Juricic, E. & Bonadonna, F. 2018b. Visual field shape and foraging ecology in diurnal raptors. *J Exp Biol* **221**.

Potier, S., Lieuvin, M., Pfaff, M. & Kelber, A. 2020a. How fast can raptors see? *Journal of Experimental Biology* **223**.

Potier, S., Mitkus, M., Bonadonna, F., Duriez, O., Isard, P. F., Dulaurent, T., Mentek, M. & Kelber, A. 2017. Eye Size, Fovea, and Foraging Ecology in Accipitriform Raptors. *Brain Behav Evol* **90**: 232-242.

Potier, S., Mitkus, M. & Kelber, A. 2020b. Visual adaptations of diurnal and nocturnal raptors. *Seminars in Cell & Developmental Biology* **106**: 116-126.

Potier, S., Roulin, A., Martin, G. R., Portugal, S. J., Bonhomme, V., Bouchet, T., de Romans, R., Meyrier, E. & Kelber, A. 2023. Binocular field configuration in owls: the role of foraging ecology. *Proceedings of the Royal Society B: Biological Sciences* **290**: 20230664.

Quast, C., Pruesse, E., Yilmaz, P., Gerken, J., Schweer, T., Yarza, P., Peplies, J. & Glöckner, F. O. 2013. The SILVA ribosomal RNA gene database project: improved data processing and web-based tools. *Nucleic Acids Res* **41**: D590-6.

Ruggeri, M., Major, J. C., Jr., McKeown, C., Knighton, R. W., Puliafito, C. A. & Jiao, S. 2010. Retinal structure of birds of prey revealed by ultra-high resolution spectral-domain optical coherence tomography. *Invest Ophthalmol Vis Sci* **51**: 5789-95.

Schmid, K. L. & Wildsoet, C. F. 1998. Assessment of visual acuity and contrast sensitivity in the chick using an optokinetic nystagmus paradigm. *Vision Research* **38**: 2629-2634.

Shi, Q. & Stell, W. K. 2013. Die Fledermaus: regarding optokinetic contrast sensitivity and light-adaptation, chicks are mice with wings. *PLoS One* **8**: e75375.

Shi, Y., Radlwimmer, F. & Yokoyama, S. 2001. Molecular genetics and the evolution of ultraviolet vision in vertebrates. *PNAS* **98**: 11731–11736.

Siitari, H., Viitala, J. & Hovi, M. 2002. Behavioural evidence for ultraviolet vision in a tetraonid species – foraging experiment with black grouse Tetrao tetrix. *Journal of Avian Biology* **33**: 199-202.

Simão, F. A., Waterhouse, R. M., Ioannidis, P., Kriventseva, E. V. & Zdobnov, E. M. 2015. BUSCO: assessing genome assembly and annotation completeness with single-copy orthologs. *Bioinformatics* **31**: 3210-2.

Song, L. & Florea, L. 2015. Rcorrector: efficient and accurate error correction for Illumina RNA-seq reads. *GigaScience* **4**: 48.

Spiegel, O., Getz, W. M. & Nathan, R. 2013. Factors Influencing Foraging Search Efficiency: Why Do Scarce Lappet-Faced Vultures Outperform Ubiquitous White-Backed Vultures? *The American Naturalist* **181**: E102-E115.

Toomey, M. B., Collins, A. M., Frederiksen, R., Cornwall, M. C., Timlin, J. A. & Corbo, J. C. 2015. A complex carotenoid palette tunes avian colour vision. *Journal of The Royal Society Interface* **12**: 20150563.

van Hazel, I., Sabouhanian, A., Day, L., Endler, K. & Chang, B. 2013. Functional characterization of spectral tuning mechanisms in the Great Bowerbird short-wavelength sensitive visual pigment (SWS1), and the origins of UV/violet vision in passerines and parrots. *BMC Evol Biol* **13**: 250.

Wagner, H., Pappe, I. & Nalbach, H. O. 2022. Optocollic responses in adult barn owls (Tyto furcata). *J Comp Physiol A Neuroethol Sens Neural Behav Physiol* **208**: 239-251.

Witter, M. S. & Cuthill, I. C. 1993. The ecological costs of avian fat storage. *Philos Trans R Soc Lond B Biol Sci* **340**: 73-92.

Wu, Y., Hadly, E. A., Teng, W., Hao, Y., Liang, W., Liu, Y. & Wang, H. 2016. Retinal transcriptome sequencing sheds light on the adaptation to nocturnal and diurnal lifestyles in raptors. *Scientific Reports* **6**: 33578.

Yokoyama, S., Tada, T., Liu, Y., Faggionato, D. & Altun, A. 2016. A simple method for studying the molecular mechanisms of ultraviolet and violet reception in vertebrates. *BMC Evol Biol* **16**: 64.